

Large Scale 3D Airborne Electromagnetic Inversion – Recent Technical Improvements.

Michael S. McMillan*
Computational Geosciences Inc
Vancouver, BC
mike@compgeoinc.com

Eldad Haber
University of British Columbia
Vancouver, BC
ehaber@eoas.ubc.ca

Dave Marchant
Computational Geosciences Inc.
Vancouver, BC
dave@compgeoinc.com

**presenting author asterisked*

SUMMARY

3D airborne electromagnetic (AEM) inversion has routinely been applied to frequency and time-domain problems over the past few years, however this research field continues to undergo rapid improvements with the implementation of new ideas and faster computational resources. To keep pace with these developments, we have rewritten our 3D AEM inversion software suite to leverage the rapid growth in parallel processing, and to create a flexible inversion framework capable of standard inversion plus many additional types: joint, cooperative or parametric, all on semi-structured octree meshes. Our resulting framework further improves recent key ideas such as the decoupling of forward meshes from the inverse mesh, to allow the forward problem to be easily distributed on separate nodes of a cluster for fast and efficient modelling of the fields.

We present two large-scale field examples, one in the frequency domain and one in the time domain. The frequency domain survey demonstrates our ability to recover thin conductors, in this case representing orogenic gold targets, across a large region (40km x 35km). The time domain example focuses on a smaller area within a larger survey area where mapping groundwater resources is the primary goal. Here the fine-scale results are compared to a 1D inversion, and we see a good correlation between the 3D and 1D results due to an approximately 1D layered-earth environment. However we see a removal of 1D artifacts in the neighbourhood of vertical conductors and topographic changes in the 3D result with the added bonus of information between lines in which decisions regarding groundwater management can be made.

Key words: electromagnetics, inversion, 3D, large-scale, airborne.

INTRODUCTION

The level of sophistication of 3D airborne electromagnetic (AEM) inversion software is under a state of constant development. Coupled with data acquisition improvements and the rise in parallel computing, the capability of large scale 3D AEM inversion modelling for both time and frequency domain data is reaching new heights. Airborne electromagnetic systems have seen a steady advancement in signal to noise ratios, allowing systems to penetrate much deeper than previously possible. This permits the detection of buried mineralization and ore bodies that would have been masked in the noise from previous systems. These modern systems also collect much more data in the form of additional time gates and multi-component measurements, and when the geology is 3D in nature, these systems rely on robust 3D inversion codes to make the best use of the recorded data. With modern data collection systems and robust 3D inversion codes, the result is, not surprisingly, higher quality and more detailed physical property models compared to prior years.

Simplified interpretation techniques such as conductivity-depth imaging (Eaton, 1998) are common and quick tools to determine approximate structure in an area. However as the complexity of data and underlying geology increases, it is more difficult to make interpretations based on such reduced-physics transformations alone. Inversion of geophysical data thus becomes a crucial component to generate an accurate earth model that ensures the recovered geophysical model satisfies the data measurements. 1D AEM inversions are routinely performed with satisfactory results for many geologic environments with roughly horizontal layered media. These include standalone 1D inversion packages such as EM1DTM/FM developed by UBC-GIF (Farquharson and Oldenburg, 1993) and 1D laterally constrained software packages such as VPEM1D (Fullagar et al., 2010). In addition, plate modelling such as Maxwell (EMIT, 2005) MultiLoop (Lamontagne et al., 1988) has achieved huge success for modelling thin conductive plate-like anomalies. While plate modelling is still often the industry standard for many geologic settings such as VMS deposits, certain approximations made to the physics have motivated hybrid methods such as voxel based parametric approaches. Once again, when the geology is strictly 3D in nature, both plate modelling and 1D assumptions can break down and full 3D modelling are required to accurately image the subsurface. These 3D models can help eliminate artifacts from 1D assumptions for example and may assist the exploration geoscientist to interpret complex 3D geologic structures.

3D AEM inversions are now routinely performed when the setting is appropriate, but the challenge of inverting modern large-scale survey areas with huge amounts of sources is ongoing. This improvement is due to two main factors. Firstly, computational resources advance in-line with Moore's Law, and secondly, algorithms are being efficiently distributed onto parallel architectures. To this end, companies such as Amazon have played a significantly role in this market by the implementation of cloud computing. This means that it is now possible for a smaller company to quickly spin up large computing systems on the cloud using parallel inversion software spread over thousands of processors. In this work we will tell the story of recent technical improvements within 3D AEM inversion, and will present results from two case studies using a frequency-domain and a time-domain system that demonstrate our current capabilities.

METHODS

At Computational Geosciences Inc., our 3D AEM software is completely written in the Julia programming language (Bezanson et al., 2012) which allows for a modular and easily parallelizable approach to the forward and inverse problem. This framework allows much more flexibility compared to previous versions of the software. Another benefit of Julia, is the just-in-time compiler nature of the language, which enables the user to edit the code without having to re-compile. The general framework and specific contents are now outlined.

To perform a forward simulation, a discretized mesh is constructed that spans the spatial domain of interest. A variety of mesh options exist, each with pros and cons, such as a regular mesh, a semi-structured mesh or an unstructured mesh. For regular meshes, they are easy to build and to view, but they have trouble discretizing complex geologic or topographic features. In addition they can be poorly conditioned in areas with large padding regions, and require many cells to cover the whole domain. For an unstructured mesh, such as one composed of tetrahedra as commonly used in finite-element modelling, the meshes are hard to generate and they can also produce potentially poorly conditioned matrices. However, in contrast to regular meshes they are efficient at discretizing complicated geologic features, bathymetry and topography. Semi-structured or octree meshes (Haber and Heldmann, 2007) represent a compromise between regular and unstructured meshing. These meshes are easier to construct compared to an unstructured orientation but are more complicated and flexible compared to regular meshing. As such, topography and geology can be well discretized but not to the same accuracy level as with tetrahedra. However the system is often better conditioned and the number of mesh cells remains relatively low. As a result, we work with semi-structured octree meshes, and a summary of the different meshes is shown below in Figure 1.

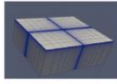
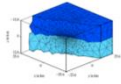
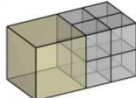
			
	Regular	Unstructured	OcTree
Meshing	✓	×	✓-
Geology	×	✓	✓-
Conditioning	×	+×	✓
DOF	×	✓	✓+

Figure 1: Pros and cons of regular, unstructured and octree meshing.

One of the main developments that has led to efficient 3D AEM codes in the past few years is decoupling the forward meshes from each transmitter/receiver pair from the inversion mesh (Haber and Schwarzbach, 2014). Figure 2 displays an example of a forward and inverse mesh for a typical AEM survey along with an emphasis for how topography is finely discretized. The forward mesh contains fine cells only in the region next to a single transmitter/receiver pair, and is perfectly nested within a single inverse mesh. This inverse mesh covers the entire survey area with fine cells near all transmitter/receiver pairs as well as near the air/earth interface to accurately represent the topography. This mesh decoupling allows the forward mesh to have a reduced number of cells (~12,500 in Figure 2a) in which to compute the electric and magnetic fields. These fields are solved according to quasi-static Maxwell's equations seen for the time-domain in Equation 1. Here \mathbf{e} represents electric fields which are solved along the edges of each mesh cell using a finite volume approach, \mathbf{h} are magnetic fields, \mathbf{s} a source vector, σ conductivity, μ magnetic susceptibility, and t represents time.

$$\begin{aligned}\nabla \times \mathbf{e} + \mu \frac{\partial \mathbf{h}}{\partial t} &= 0 \\ \nabla \times \mathbf{h} - \sigma \mathbf{e} &= \mathbf{s}\end{aligned}\tag{1}$$

These fields are required for the model update step on the inverse mesh, which has many more cells (~4,000,000 in Figure 2b). For a typical AEM survey with thousands or more transmitter/receiver positions, the forward simulation is easily parallelized with such a mesh decoupling approach. In this way, the fields from each forward mesh can be computed on separate computer nodes and assembled for the Gauss-Newton update step. Due to the modular nature of the Julia framework, once the meshing has been completed, the code can call the forward model operators in either the frequency or time-domain. Furthermore, this step can handle as many time channels and frequencies as necessary, but additionally can easily implement multiple transmitter orientations and waveforms for each data point. For such systems as SkyTEM (Sørensen and Auken, 2004) that have a dual-pulse, this modular approach makes performing a joint inversion of both pulses of data a simplistic task. It is also trivial to perform a parametric inversion or a hybrid parametric inversion (McMillan et al., 2015) in both the time and frequency domain as it just requires an additional layer of parametrization and derivatives using the same forward operators and inversion framework as the voxel inversions. A visual example of the parametric and hybrid parametric is displayed in Figure 3.

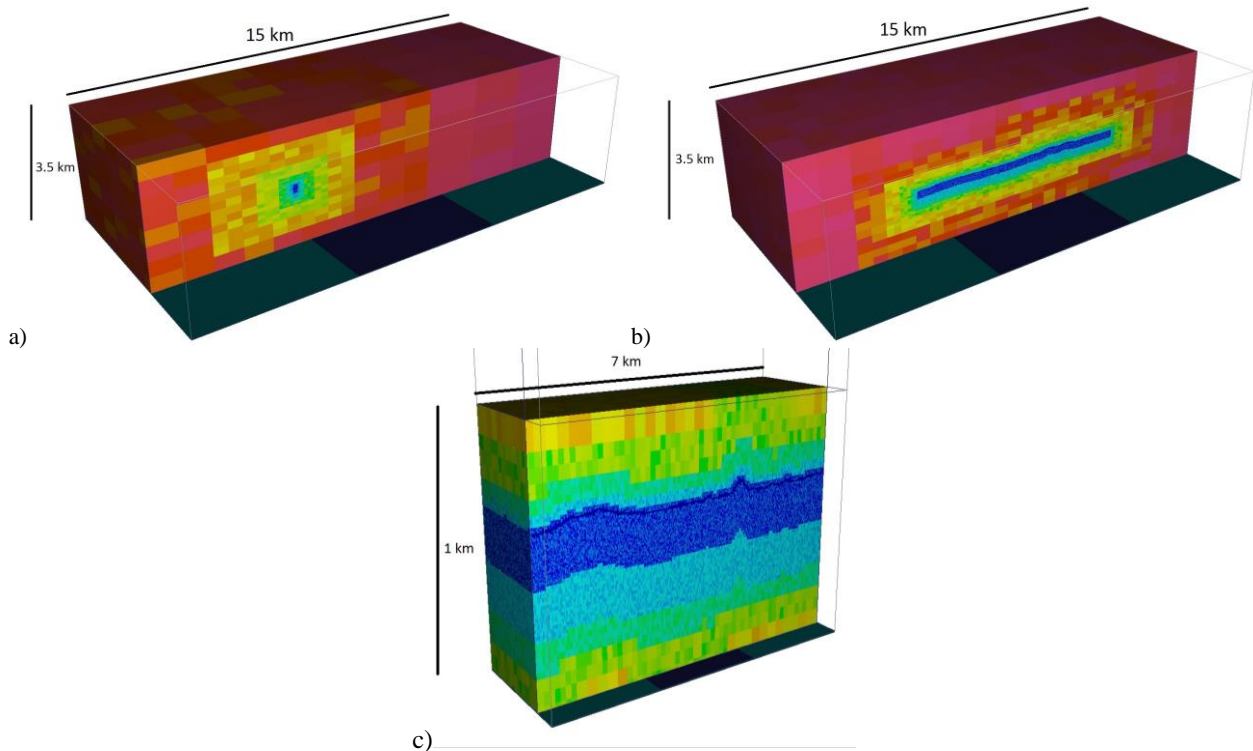


Figure 2: Forward and inversion AEM octree meshes. Finest cell size = 7 m x 7 m x 3.5 m. Colours indicate an approximation of the cell volume. a) Forward model mesh finely discretized near a single transmitter / receiver pair. Total number of cells = 12,574. b) Inversion mesh finely discretized over entire survey region. Total number of cells = 3,901,942. c) Close up on inverse mesh with a vertical exaggeration = 5 to see the additional layer of fine cells discretizing the topography.

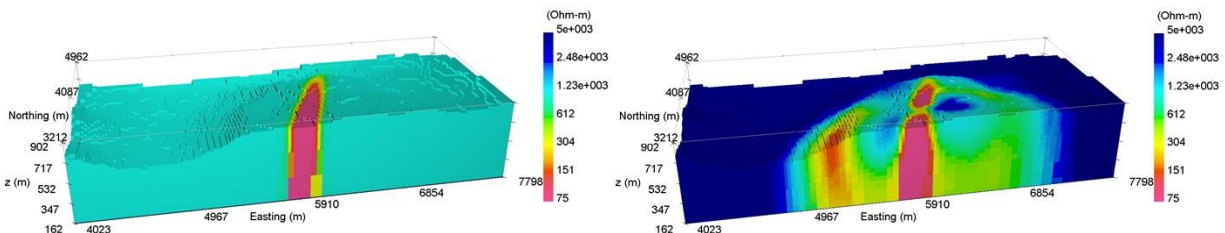


Figure 3: Example of time-domain AEM parametric and hybrid inversion models. Left) Parametric model outlining the best fitting skewed Gaussian ellipsoid representing the primary target of interest. Right) Hybrid model using the parametric model as a starting guess for the voxel inversion to fill in remaining features missed by the parametric stage.

RESULTS

Frequency-domain RESOLVE

We present two brief field examples to showcase the versatility of the inversion framework for large-scale problems. The first is for a frequency domain RESOLVE (Viezzoli et al., 2009) survey from 2016 over the Committee Bay greenstone belt in Nunavut, Canada. This region, shown in Figure 4 is an active exploration environment for orogenic and banded-iron hosted gold. The survey goal was to identify conductive komatiite units that could potentially host mineralization in the area (Kerswill, 1996). An airborne survey was an obvious choice in this region as large swathes of land needed to be covered. The background rocks at Committee Bay are highly resistive, and a frequency domain survey was chosen due to its ability to collect high resolution near-surface data at high frequencies. In addition to mapping komatiites and other conductive lithologies of interest such as banded iron formations, the RESOLVE survey also highlighted important geologic structures in the region. These faults and fracture networks can provide useful information in order to understand the potential fluid pathways that generated the mineralizing events. In total, 6000 line-km of data were collected over roughly a 40 km x 35 km area, with a 200 m line spacing. Six frequencies were acquired between 400 Hz and 115,000 Hz with five coplanar orientations and one coaxial orientation at 3300 Hz. Over 60,000 source locations, each with six frequencies, are incorporated into the inversion using an octree mesh of ~2,000,000 cells with forward meshes of ~10,000 cells each. The smallest cell size is 70m x 70m x 20m in this example. The inversion took ~ 55 hrs to run on 40 cores with an Intel Xeon E5-2690 v3 processor, 2.60 GHz and 256 Gbs of memory.



Figure 4: Location of 2016 frequency-domain RESOLVE survey over Committee Bay greenstone belt, Nunavut, Canada.

The quadrature component of the secondary vertical magnetic field from 8200 Hz is shown in the left panel of Figure 5. This data map portrays many thin linear conductive features of interest. The corresponding inversion of the entire data set is shown in the right panel of Figure 5 at an approximate depth slice of 25m below surface, and the linear conductors are well captured in the inversion. Extensive drill testing occurred during the summer of 2017 and some ground truth for these models should be available soon to provide geologic and physical property information which can be used to further constrain and improve the results.

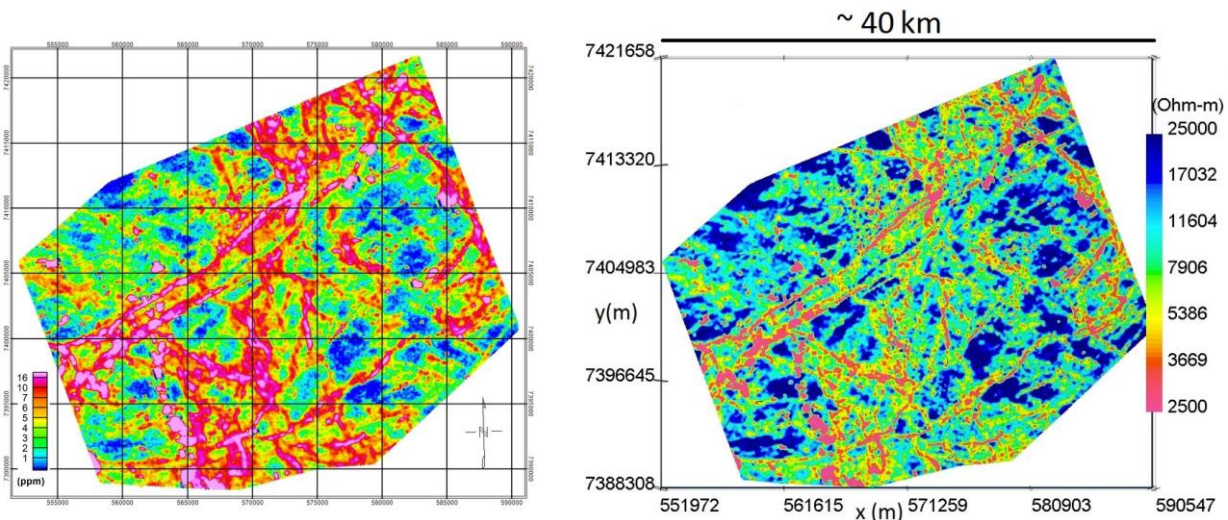


Figure 5: AEM Frequency domain data and 3D inversion over an orogenic gold exploration area in Nunavut, Canada. Left) z-component Magnetic-field, quadrature component, 8200 Hz. Right) 3D inversion model at an approximate depth of 25 m.

Time-domain SKYTEM

The second field example is from a 2015 time-domain SKYTEM example over an area in the North-East corner of Western Australia, where Geoscience Australia was doing a groundwater resource mapping initiative. The location of the survey is shown in the left panel of Figure 6. In total close to 3000 line-km of data was collected with a 400m line spacing over a 40 km x 20 km area. The entirety of the survey was inverted in 3D with a smallest mesh cell size of 12m x 12m x 6m. However we will zoom in to a smaller test area with 6 lines of data and a total of 1177 transmitter/receiver pairs. The forward meshes each had roughly ~12,000 cells while the inversion mesh had ~3.9 million cells, each with a smallest cell size of 7m x 7m x 3.5m. The inversion took ~48 hrs to run on 48 cores with an Intel Xeon E5-2690 v3 processor, 2.60 GHz and 256 Gbs of memory. Observed data from the high-moment dBz/dt component at 458 μ s is shown in the center panel of Figure 6 with corresponding predicted data from the inversion in the right panel. A joint inversion of the low and high moment data was performed, and equally good data fits are also produced for the low moment but are not shown. In Figure 7 the 1D and 3D joint inversion results are shown for a 2D cross-section over a central line of data. The joint 1D inversion, completed by Niels Christensen and the team at Aarhus University, is shown in the left panel. In this nearly-flat 1D environment with a large spacing between adjacent lines (400m), the 1D approximation is fairly accurate and is a good comparison for the 3D code. Our joint 3D results are shown in the right panel. Overall the comparisons are quite similar. The 1D code is able to resolve the near-surface layering to a better degree due to smaller cells near the air/earth interface, however, any potential pant-leg artifacts due to near-vertical conductors or topography effects are removed in the 3D result. Another added benefit to the 3D model is that it resolves the conductivity in between lines, hence, cutoff volumes can be produced to display 3D boundaries such as the one evident in Figure 8. Here a 0.02 S/m cutoff is applied and only more resistive cells are shown. This potential freshwater front can be used to identify fresh water boundaries

throughout the 3D volume. Future 3D inversions can aim to reduce the cell size near the air/earth interface to further improve the results.

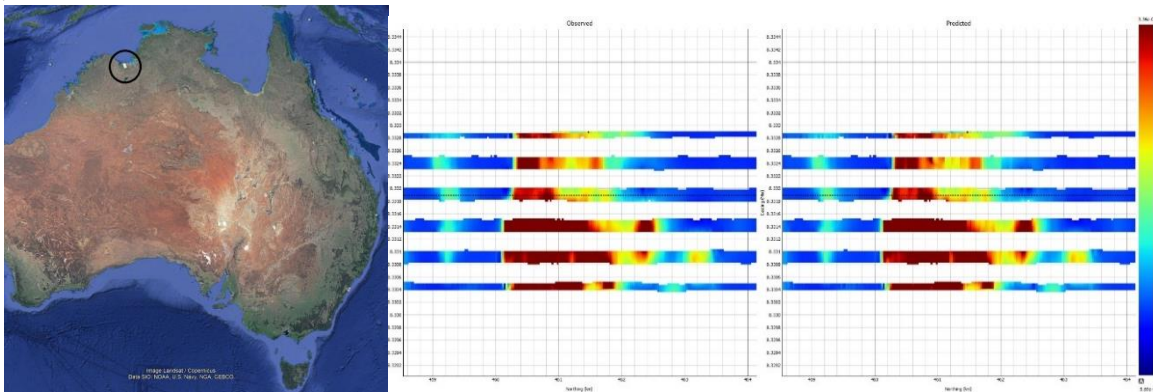


Figure 6: Left) Location of time-domain AEM SKYTEM survey. Center) Observed dBz/dt for high moment data at 458 μ s. Right) Predicted dBz/dt for high moment data at 458 μ s.

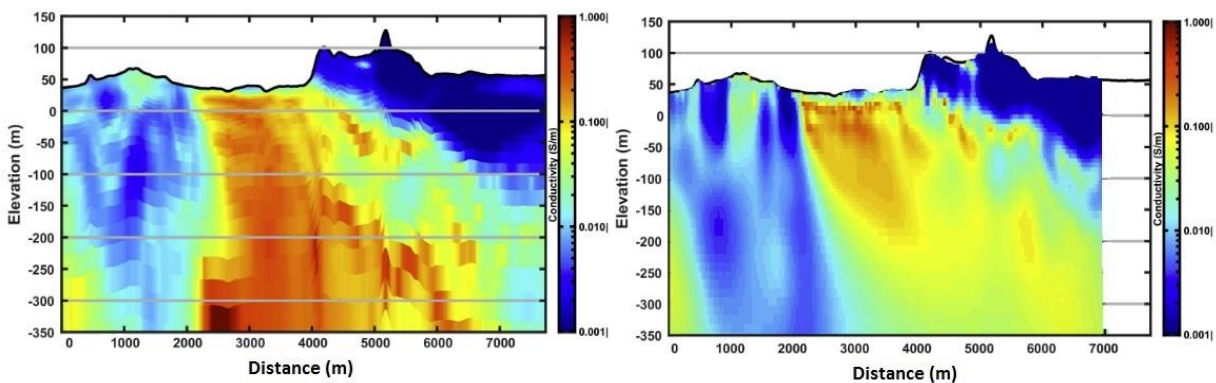


Figure 7: 1D and 3D AEM inversion across a line of data in a water management region in Australia. Left) 1D. Right) 3D. Note there is a vertical exaggeration of 7 times which distorts the look of the topography.

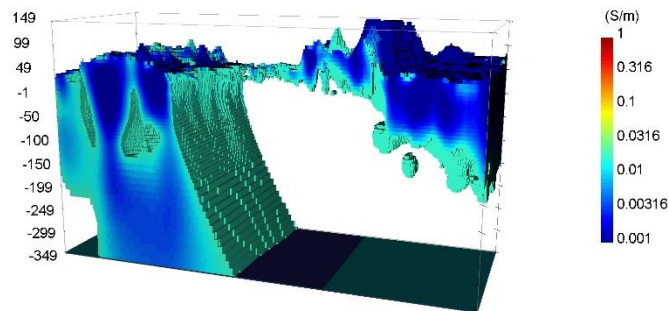


Figure 8: 0.02 S/m cutoff through 3D inversion model. Vertical exaggeration = 7.

CONCLUSIONS

Efficient large-scale 3D airborne electromagnetic inversion is a continually evolving problem. Every year computer processor speed and access to multiple-core machines improves which allows for larger and larger problems to be solved. Re-formulating the forward and inverse problem over the past couple years with the mesh decoupling approach in a new language such as Julia has allowed the code to be easily parallelized to take full advantage of these technological developments. This enables an easy coding of both frequency and time-domain problems using joint, parametric and conventional voxel style inversions with the flexibility to add new styles of inversion in the future. With semi-structured meshes such as octrees, the overall number of cells in the can remain relatively small compared to regular tensor meshes over the same spatial domain while still discretizing areas of interest with fine resolution.

We presented two large-scale field examples, the first being a frequency-domain survey in the Canadian Arctic, where a RESOLVE survey was inverted. The resulting model highlighted near-surface near-vertical conductors which are potential targets for orogenic gold mineralization in the region. The second example was from a ground-water mapping initiative in Western Australia where a SKYTEM survey was inverted. A joint inversion of the high and low moment was performed over the whole region and again over a smaller test region with finer cells. In this test region the 3D inversion results compared nicely to the 1D results, with some improvements in regions with vertical conductive anomalies and significant topography changes. The 3D result also has the inherent benefit of creating 3D volumes across the whole region that can also be used to isolate potential groundwater interfaces.

ACKNOWLEDGMENTS

Thank you to Auryn Resources and Geoscience Australia for permission to present the field examples.

REFERENCES

- Bezanson, J., Karpinski, S., Shah, V.B., and Edelman, A., 2012, Julia: A Fast Dynamic Language for Technical Computing: arXiv preprint arXiv:1209.5145.
- Eaton, P., 1998, Application of an improved technique for interpreting transient electromagnetic data: *Exploration Geophysics*, 29, 175–183.
- EMIT, 2005, Maxwell 4.0: Modeling, presentation and visualization of EM and electrical geophysical data: Technical report.
- Farquharson, G., and Oldenburg, D.W., 1993, Inversion of time-domain electromagnetic data for a horizontally layered Earth: *Geophysical Journal International*, 114, 433–442.
- Fullagar, P.K., Urbancich, J., and Pears, G.A., 2010, Geologically-constrained 1D TEM inversion: ASEG Expanded Abstract.
- Haber, E., and Heldmann, S., 2007, An octree multigrid method for quasi-static Maxwell's equations with highly discontinuous coefficients: *Journal of Computational Physics*, 223(2), 783-796.
- Haber, E., and Schwarzbach, C., 2014, Parallel inversion of large-scale airborne time-domain electromagnetic data with multiple OcTree meshes: *Inverse Problems*, 30, 1–28.
- Kerswill, J.A., 1996, Iron-formation-hosted stratabound gold: *Geology of Canadian mineral deposit types. Geology of Canada*, 8, 367–382.
- Lamontagne, Y., Macnae, J., and Polzer, B., 1988, Multiple conductor modeling using program MultiLoop: 58th Meeting, SEG, Anaheim, Expanded Abstracts, 237-240.
- McMillan, M.S., Schwarzbach, C., Haber, E., and Oldenburg, D.W., 2015, 3D parametric hybrid inversion of time-domain airborne electromagnetic data: *Geophysics*, 80, K25–K36.
- Sørensen, K.I., and Auken, E., 2004, SkyTEM a new high-resolution helicopter transient electromagnetic system: *Exploration Geophysics*, 35, 194–202.
- Viezzoli, A., Auken, E., and Munday, T., 2009, Spatially constrained inversion for quasi 3D modelling of airborne electromagnetic data an application for environmental assessment in the Lower Murray Region of South Australia: *Exploration Geophysics*, 40, 173–183.